Engineering," Vol. 10, p. 144, Plenum Press, New York (1965).
14. Myers, A. L., and J. M. Prausnitz, *A.I.Ch.E. J.*, **11**, 121 (1965).
15. Loebenstein, W. V., and V. R. Deitz, *J. Res. NBS*, **46**, 51 (1951).
16. Vermeulen, T., "Advances in Chemical Engineering," Vol. 2, p. 147, Academic Press, New York (1958).
17. Klotz, I., *Chem. Rev.*, **39**, 241 (1946).
18. Eagleton, L. C., and H. Bliss, *Chem. Eng. Progr.*, **49**, 543 (1953).
19. Glueckauf, E., and J. Coates, cited in "Advances in Chemical Engineering," J. W. Hoopes, Jr., and T. B. Drew, eds.; Vol. 2, Academic Press, New York (1958).
20. Gupta, A. S., and George Thodos, *Chem. Eng. Progr.*, **58**, 58 (1962).
21. Brilliantov, N. A., and A. B. Fradkov, *Soviet Phys.-Tech. Phys.*, **2**, No. 10, 2239 (1957); English translation of *J. Tech. Phys.* (*USSR*), **27**, No. 10, 2404 (1957).

Manuscript received May 10, 1965; revision received August 12, 1965; paper accepted August 16, 1965. Paper presented at A.I.Ch.E. San Francisco meeting.

Laminar Converging Flow of Dilute Polymer Solutions in Conical Sections:

Part I. Viscosity Data, New Viscosity Model, Tube Flow Solution

J. L. SUTTERBY

University of Wisconsin, Madison, Wisconsin

This investigation is reported in two parts. Necessary background information is introduced in Part I. The converging flow investigation proper is described in Part II (*18*).

In Part I, viscosity data are presented for polymer solutions used in the converging flow experiment. These data are fitted with a new three-parameter viscosity model which fits the data better than previous three-parameter models. (The viscosity model parameters are used in Part II to characterize rheological behavior of the polymer solutions in the converging flow experiment.) The corresponding relationship between flow rate and pressure drop for laminar flow in cylindrical tubes is derived. (In Part II this relationship is used in deriving an analogous relationship for slow non-Newtonian flow in conical sections.)

The primary purpose of Part I is to provide background information for Part II. However, the new viscosity model and the tube flow relationship are of some interest in themselves. The new viscosity model should prove useful for describing viscosity data of a variety of polymer solutions and polymer melts. A simple procedure for fitting the model to viscosity data is described. The tube flow relationship can be used for predicting pressure losses once the viscosity model parameters have been determined. Conversely, it can be used for determining the viscosity model parameters from tube flow data.

Polymer solutions and polymer melts exhibit several types of rheological phenomena. These include non-Newtonian viscosity, normal stresses in steady shear flow, and various time-dependent elastic effects. In some applications viscosity data alone give an adequate rheological description of such viscoelastic fluids. For example, viscosity data are sufficient for establishing the flow rate vs. pressure drop relationship for steady laminar flow in tubes—one of the simple viscometric flows having only one velocity component. In nonviscometric flows (for example, flow in conduits with varying cross section, flow in packed beds, turbulent flows), viscosity data may not be sufficient for establishing the flow rate vs. pressure drop relationship. The complexity of the fluid evidenced by normal stresses and time-dependent elastic effects may influence this relationship.

An a priori estimate of the magnitude of this effect cannot be made because little is known about nonviscometric flows. This investigation (*17*) provides information for one particular nonviscometric flow, namely, laminar converging flow in conical sections.

If one knew how to characterize completely the rheological behavior of viscoelastic fluids, the problem would be solved, at least in principle. In simple cases one might be able to derive the flow rate vs. pressure drop relationship. In more complex ones, consideration of the dimensionless form of the flow equations would indicate suitable dimensionless groups for correlating experimental data and would also indicate under what conditions order-of-magnitude simplifications could be made. Unfortunately, it is not yet known how to characterize completely the behavior of viscoelastic fluids. Many rheologists are currently occupied with this problem. A recent text by Lodge (*8*) provides an excellent introduction to this work.

The approach taken in this investigation was to assume that viscosity data were sufficient for establishing the flow rate vs. pressure drop relationship in the converging flow experiment. Good agreement between experiment and theory based on this hypothesis would verify the hypothesis, provided, of course, that the investigation were carefully done. A large discrepancy would refute the hypothesis, indicating need for additional rheological data. A more extensive investigation would then be required to determine what additional rheological data were needed and how they should be employed.

The investigation is reported in two parts. Necessary background information is introduced in Part I (this

J. L. Sutterby is at Virginia Polytechnic Institute, Blacksburg, Virginia.

TABLE 1. SEVERAL VISCOSITY MODELS (*14, 13, 6, 15*)

Originator	Model	Parameters
Ostwald-de Waele	$\eta = m\lvert\Delta\rvert^{n-1}$	m, n
Ellis	$\eta = \eta_o/(1 + \lvert\tau/\tau_{1/2}\rvert^{\alpha-1})$	$\eta_o, \tau_{1/2}, \alpha$
Meter	$\eta = \eta_o\left[\frac{1 + \lvert\tau/\tau_m\rvert^{\alpha-1}(\eta_\infty/\eta_o)}{1 + \lvert\tau/\tau_m\rvert^{\alpha-1}}\right]$	$\eta_o, \eta_\infty, \tau_m, \alpha$
Eyring	$\eta = \eta_o\frac{\text{arc sinh }(B\Delta)}{(B\Delta)}$	η_o, B
Powell-Eyring	$\eta = \eta_\infty + (\eta_o - \eta_\infty)\frac{\text{arc sinh }(B\Delta)}{(B\Delta)}$	η_o, η_∞, B
Seely	$\eta = \eta_\infty + (\eta_o - \eta_\infty)e^{-\sigma\tau}$	$\eta_o, \eta_\infty, \sigma$

paper). The converging flow investigation proper is described in Part II (*18*).

GENERALIZED NEWTONIAN CONSTITUTIVE EQUATION (3)

The generalized Newtonian equation is a relatively simple constitutive equation which can describe non-Newtonian viscosity but not normal stresses or time-dependent elastic effects. It may be written as

$$\bar{\tau} = -\eta\bar{\Delta} \tag{1}$$

For incompressible fluids, η may depend on the second and third invariants of $\bar{\Delta}$ (or of $\bar{\tau}$). These invariants are defined as

$$II_\Delta = \sum_{ij}\Delta_{ij}\Delta_{ji} \tag{2}$$

$$III_\Delta = \text{determinant of the } \bar{\Delta} \text{ matrix} \tag{3}$$

The Δ_{ij} are tabulated in rectangular, cylindrical, and spherical coordinates on pages 88 to 90 of reference 3. In viscometric flows, III_Δ vanishes and hence has no effect on η. In nonviscometric flows the dependence of η on III_Δ is not known. It is customary to neglect any such dependence and assume that η is a function of II_Δ only.

In viscometric flows, Equation (1) reduces to

$$\tau = -\eta\Delta \tag{4}$$

For polymer solutions and polymer melts, one commonly observes that η approaches a limiting value η_o as Δ approaches zero, and that η approaches another limiting value η_∞ (less than η_o) as Δ becomes very large. For intermediate Δ, one often observes that log η is a linear function of log Δ for a wide range of Δ. The latter characteristic is called *power law behavior.*

A number of models have been proposed to describe viscosity data. Several are listed in Table 1. These models are merely mathematical functions of τ or Δ which conform to one or more of the characteristics of viscosity data noted above. Each model contains adjustable parameters which are determined by curve fitting the model to viscosity data. One hopes that these parameters can be used to characterize the behavior of the fluid in nonviscometric flows. The usual approach is to convert the η model to tensorially invariant form by replacing Δ by $(\frac{1}{2}\ II_\Delta)^{1/2}$ [or τ by $(\frac{1}{2}\ II_\tau)^{1/2}$]. Equation (1) is then substituted into the equations of motion and energy (see for example, reference 3). In simple applications, these equations can be solved. In more complex ones, dimensional analysis will indicate suitable dimensionless groups for correlating experimental data. It should be emphasized that this procedure does not account for normal stresses, time-dependent elastic effects, or the effect of III_Δ on η. Hence, it may not be applied indiscriminately. Several successful applications (including this one) were recently cited by Bird (*4*).

Viscosity Models

Characteristics of models listed in Table 1 are described below.

The Ostwald-de Waele or power law model (two parameters) predicts a linear relationship between log η and log Δ. It cannot describe η_o or η_∞ and hence is applicable only for intermediate shear rates.

The Ellis model (three parameters) can describe η_o but not η_∞. For large Δ it predicts a linear relationship between log η and log Δ. This model is applicable for low and intermediate shear rates. Mathematical solutions for flow of an Ellis model fluid were recently catalogued by Matsuhisa and Bird (*9*).

The Powell-Eyring model (three parameters), Seely model (three parameters), and Meter model (four parameters) are adapted for fitting viscosity data over the entire range of shear rates. All three can describe η_o and η_∞. The Powell-Eyring and Seely models may not do a good job at intermediate shear rates, particularly when the data approximate power law behavior over an extended range of Δ.

One final observation concerning the Ellis and Meter models: As parameter α approaches 1, $1/\tau_{1/2}$, and $1/\tau_m$ must approach zero. Otherwise these models do not reduce to the proper Newtonian limit ($\eta = \eta_o$) as α approaches 1.

NEW VISCOSITY MODEL

A new viscosity model was proposed recently (*17*)

$$\eta = \eta_o\left[\frac{\text{arc sinh }(B\Delta)}{(B\Delta)}\right]^A \tag{5}$$

in which η_o, A, and B are positive parameters. Parameter η_o has the units of viscosity; A is dimensionless; B is a characteristic time. Figure 1 shows the general shape of viscosity curves predicted by Equation (5). The viscosity η approaches a limiting value η_o as Δ approaches zero. For large Δ, the relationship between log η and log Δ becomes linear with slope $-A$. Parameter B specifies the value of Δ for which η begins to drop off rapidly from η_o. This model should prove useful for describing viscosity data of a variety of polymer solutions and polymer melts for shear rates varying between zero and some indefinite upper limit. Equation (5) cannot describe η_∞. This is not necessarily a defect, since for many systems η approaches η_∞ at extremely high shear rates rarely encountered in practice. In any case, the following generalization of Equation (5) can describe η_∞ as well as η_o:

$$\eta = \eta_\infty + (\eta_o - \eta_\infty)\left[\frac{\text{arc sinh }(B\Delta)}{(B\Delta)}\right]^A \tag{6}$$

Equation (6) should prove useful for describing viscosity data over the entire range $\eta_o \geqq \eta \geqq \eta_\infty$.

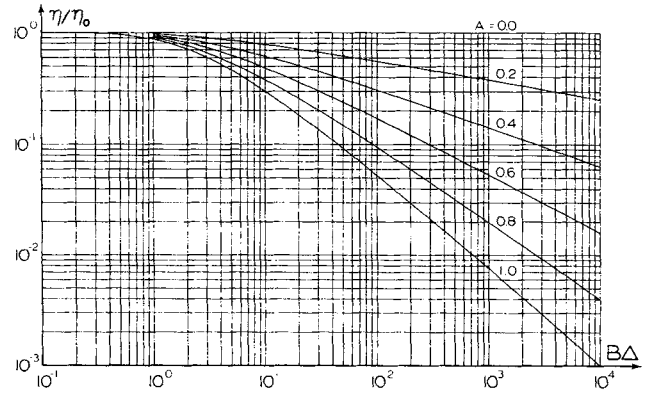

Fig. 1. Master plot of η/η_0 calculated in accordance with Equation (5). Table B-3 of reference 17 contains entries for plotting nine interpolation curves between each pair of curves shown here.

When $A = 0$, Equations (5) and (6) both predict Newtonian behavior ($\eta = \eta_0$). When $A = 1$, Equation (5) reduces to the Eyring model, and Equation (6) reduces to the Powell-Eyring model. The Eyring models have some theoretical basis. However, no theoretical significance is claimed for Equations (5) and (6). It is merely suggested that models of this type are flexible curve fitting devices.

Curve Fitting Procedure

It is assumed that viscosity data have been reduced to the form η vs. Δ and that it is desired to describe these data by means of viscosity model (5). A simple procedure for determining parameters η_0, A, and B is described below.

Table B-3 of reference 17 is a table of values of the function η/η_0 defined by Equation (5). Entries are given for thirty-six values of $B\Delta$ (at intervals of approximately 1/5 logarithmic cycle in the range $0.01 \leq B\Delta \leq 100{,}000$) and for fifty-one values of A (at intervals of 0.02 in the range $0 \leq A \leq 1$). From this table a master plot of log (η/η_0) vs. log $(B\Delta)$ is prepared with curves for several values of A. Such a master plot is shown in Figure 1. The viscosity data are plotted as log η vs. log Δ on a translucent sheet of graph paper of the same scale as that of the master plot. This data plot is superimposed on the master plot and moved about (keeping the coordinate axes of the two plots parallel) to find the curve of the master plot which best fits the viscosity data Parameter A is read from this curve. Parameter η_0 is read from the ordinate η on the data plot which coincides with the $\eta/\eta_0 = 1$ ordinate on the master plot. Similarly, parameter B is read from the abscissa $B\Delta$ on the master plot which coincides with the $\Delta = 1$ abscissa on the viscosity plot.

Once the master plot has been prepared, the parameters for a number of fluids can be determined quickly and easily. A distinct advantage of this method is that one can see directly how well the model fits the viscosity data. A similar procedure for the Ellis model was recently described by Bird (9).

VISCOSITY DATA

The test fluids in the converging flow experiment were three aqueous solutions of Natrosol 250 H hydroxyethyl cellulose. Their nominal concentrations were 0.3, 0.5, and 0.7% by weight. Cone-and-plate and falling-sphere viscometer data were taken for each solution.

Cone-and-Plate Viscometer Data

The basic viscometer was a Ferranti-Shirley cone-and-plate viscometer. In this instrument (10, 11) the test fluid is sheared between a rotating cone and a stationary plate. Temperature is maintained constant by circulating water from a constant temperature bath through a labyrinth in the plate. The measured variables are Ω and T. The formulas for calculating shear stress, viscosity, and shear rate are of form [see, for example, Slattery (16)]

$$\tau = K_\tau T \tag{7}$$

$$\eta = K_\eta (T/\Omega) \tag{8}$$

$$\Delta = (K_\tau/K_\eta)\Omega \tag{9}$$

in which K_τ and K_η are known functions of the cone slant height and the angle between the cone and plate. In this investigation, K_η was measured by calibrating the instrument with National Bureau of Standards oil L according to the procedure outlined by Biery and Huppler (2).

Falling-Sphere Viscometer Data

Falling-sphere data were taken in order to estimate η_0, the viscosity at zero shear rate. A cylinder (diameter D) filled with the test fluid (density ρ) was mounted in a constant temperature bath. Tiny ruby or glass spheres (diameter d, density ρ_s) were allowed to fall from rest along the axis of the cylinder. The terminal velocity of fall (v_t) was measured.

Viscosities were calculated according to the formula

$$\eta = \eta_s/K \tag{10}$$

in which $\eta_s = d^2(\rho_s - \rho)g/18\, v_t$ is the classic Stokes' law expression [see, for example, Lamb (7)], and K (≥ 1) is a correction which accounts for boundary and inertial effects.* The correction K is a function of diameter ratio d/D and Reynolds number $N_{Re} = d\, v_t\, \rho/\eta$. In this investigation the maximum values of d/D and N_{Re} were 0.022 and 0.7, respectively. For $N_{Re} < 0.1$, K was calculated according to the Faxén equation [see, for example, Bacon (1)] which reduces to the following form for these small values of d/D and N_{Re}:

$$1/K = 1 - 2.10\,(d/D) \tag{11}$$

For $N_{Re} > 0.1$, K was read from an empirical correlation of form K = function of $(d/D, N_{Re})$ based on data by McPherson (12).

For each Natrosol solution, viscosities were calculated according to Equation (10) for at least three sizes of spheres. These viscosities were plotted as η vs. $3\, v_t/d$. The desired limiting value η_0 was estimated by drawing a straight line through the points of this plot and extrapolating to $3\, v_t/d = 0$. This extrapolation was not drastic. The correction introduced by the extrapolation was never greater than 8%.

TREATMENT OF THE VISCOSITY DATA

Viscosity data for each Natrosol solution are plotted in Figure 2. Falling sphere estimates of η_0 are indicated by horizontal lines. The cone-and-plate data are plotted as discrete points. These points fall very nearly on straight lines (power law behavior). Cone-and-plate data could not be taken at sufficiently high shear rates for measuring values of η_∞. Two sets of data are shown for each solution. One set was measured before the converging flow experiment, the other after.

One might reasonably ask whether the high shear-rate data were affected by viscous heating. This possibility was considered. Thermocouples mounted in the plate of the viscometer in contact with the test fluid were used to

* Equation (10) is strictly applicable only to Newtonian fluids. Natrosol solutions are non-Newtonian. But for low shear rates (as in the falling sphere measurement) they behave very nearly like Newtonian fluids with viscosities near η_0.

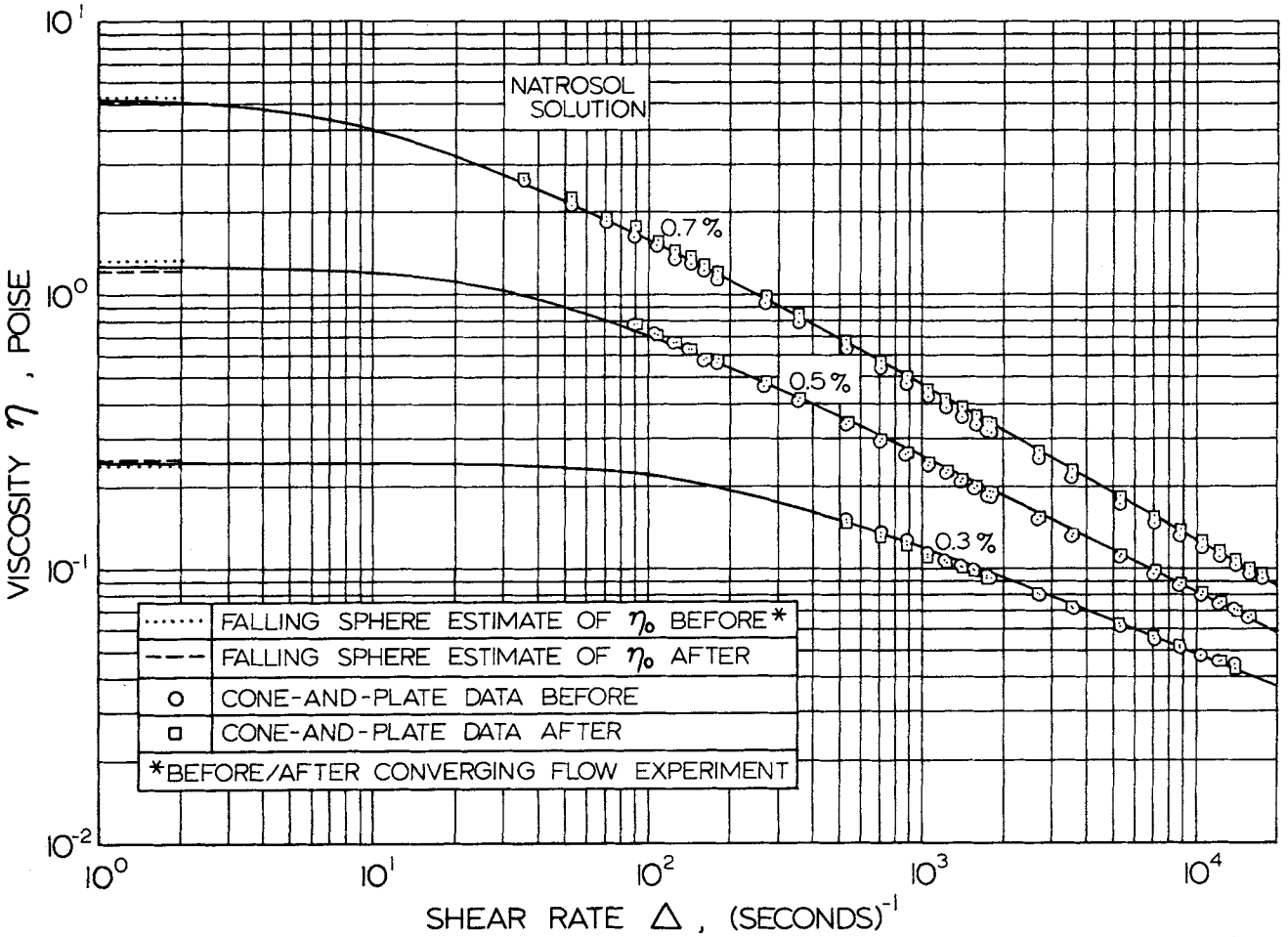

Fig. 2. Viscosity data at 25°C. for aqueous solutions of Natrosol 250 *H*. The curves are drawn in accordance with the new viscosity model of Equation (5). Corresponding parameters are recorded in Table 2.

monitor the temperature. No temperature rise due to viscous heating could be detected, even for the most viscous solution (0.7% Natrosol) at the highest shear rate (20,000 sec.$^{-1}$). A quantitative estimate of the viscous heating effect was calculated according to equation 55 of the analysis by Turian (*20*) (equation 4.2-9 of alternate reference *19*). The temperature dependence of viscosity required for this calculation was determined from viscosity data at 20°, 25°, 30°C. recorded in Table F-6 of reference *17*. The calculated viscous heating correction for the most viscous solution at the highest shear rate was only 0.3%.

Curve Fitting of Models to the Data

The viscosity data in Figure 2 have been fitted by the two-parameter Ostwald-de Waele model; by the three-parameter Ellis, Powell-Eyring, and Seely models; and by the new three-parameter model of Equation (5).

In each of the three-parameter models, parameter η_o was taken to be the experimental value determined from falling-sphere data. The two remaining parameters in each model were determined by curve fitting. The curve-fitting procedure for the new model of Equation (5) was outlined earlier in this paper. Similar procedures were followed for the Ellis, Powell-Eyring, and Seely models. For the Ellis model, the master plot was of form log (η/η_o) vs. log $(\tau/\tau_{1/2})$ with curves for several values of α. The data plot was of form log η vs. log τ. For the Powell-Eyring model, the master plot was of form log (η/η_o) vs. log $(B\Delta)$ with curves for several values of η_∞/η_o. The data plot was of form log η vs. log Δ. For the Seely model, the master plot was of form log (η/η_o) vs. log $(\sigma\tau)$ with curves for several values of η_∞/η_o. The data plot was of form log η vs. log τ. Since experimental values of η_∞ were not available, η_∞ was treated merely as an adjustable

Table 2. Viscosity Model Parameters for Aqueous Natrosol Solution at 25°C.

Ostwald-de Waele model

Concentration, wt. %	m, g./(cm.)(sec.$^{s-n}$)	$-(n-1)$, dimensionless	Range of Δ, sec.$^{-1}$
0.3	1.544	0.374	500-20,000
0.5	6.83	0.479	100-20,000
0.7	20.0	0.548	50-20,000

Ellis model

Concentration, wt. %	η_o, poise	$\tau_{1/2}$, dynes/sq. cm.	$\alpha-1$, dimensionless	Range of Δ, sec.$^{-1}$
0.3	0.245	107.0	0.9	0-20,000
0.5	1.26	87.0	1.2	0-20,000
0.7	5.10	90.2	1.4	0-20,000

New model, Equation (5)

Concentration, wt. %	η_o, poise	A, dimensionless	B, sec.	Range of Δ, sec.$^{-1}$
0.3	0.245	0.50	0.014	0-20,000
0.5	1.26	0.60	0.068	0-20,000
0.7	5.10	0.66	0.225	0-20,000

parameter in the curve-fitting procedures for the Powell-Eyring and Seely models.

As one might anticipate from the nature of these viscosity data, the new model and the Ellis model give better curve fits than do the Powell-Eyring and Seely models. Curves drawn in Figure 2 show the fit obtained with the new model. Maximum errors in fitting data for the 0.7% Natrosol solution are of the order ± 4% for the new model, ± 7% for the Ellis model, ± 19% for the Powell-Eyring model, and ± 30% for the Seely model. The Ostwald-deWaele model gives an excellent fit of the cone-and-plate data but, of course, cannot describe η_o.

Parameters for the Ostwald-de Waele model, the Ellis model, and the new model of Equation (5) are recorded in Table 2.

FLOW RATE VS. PRESSURE DROP RELATIONSHIP FOR LAMINAR TUBE FLOW

Consider the fully developed laminar flow of an incompressible fluid in a cylindrical tube. The geometry is sketched in Figure 3. It is assumed that the fluid is of generalized Newtonian type. Then the shear stress τ, viscosity η, and shear rate Δ are related as follows:

$$\tau = -\eta\,\Delta \equiv \eta\,\gamma \tag{12}$$

Integration of the equation of motion yields the following expression for the axial pressure gradient. (The equation of motion is given in cylindrical coordinates on page 85 of reference 3.)

$$-\frac{dP}{dZ} = \frac{2\tau}{r} \tag{13}$$

Here $P = p + \rho g Z \cos\beta$. The term $-\rho g Z \cos\beta$ is the hydrostatic pressure with respect to a horizontal datum plane through the origin $Z = 0$. Expression (12) for τ may be substituted into Equation (13) to obtain

$$-\frac{dP}{dZ} = \frac{2\eta\gamma}{r} = \frac{2\eta_R\gamma_R}{R} \tag{14}$$

The volumetric flow rate Q is defined as

$$Q = \int_o^R V_z\, 2\pi r\, dr \tag{15}$$

As outlined on page 70 of reference 3, this expression may be integrated by parts twice in succession to obtain the following equation. (The boundary condition $V_z = 0$ at $r = R$ is applied following the first integration.)

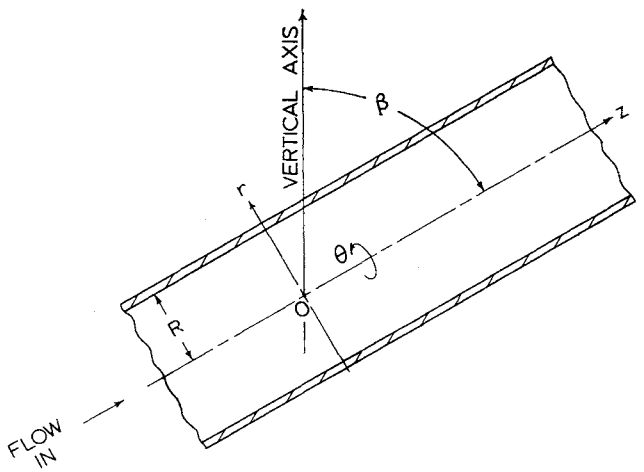

Fig. 3. Flow in a cylindrical tube. Cylindrical coordinates are r, θ, Z. The tube radius is R. The angle between the positive Z axis and an axis directed vertically upward is β.

$$Q = \frac{\pi}{3}\left(R^3\gamma_R - \int_o^{\gamma_R} r^3\, d\gamma\right) \tag{16}$$

Equation (14) is next solved for r and the resulting expression substituted into Equation (16) to obtain

$$Q = \frac{\pi}{3}\left[R^3\gamma_R - R^3\int_o^{\gamma_R}\left(\frac{\eta\gamma}{\eta_R\gamma_R}\right)^3 d\gamma\right] \tag{17}$$

Equations (14) and (17) for the pressure gradient and volumetric flow rate are valid for any fluid of generalized Newtonian type.

It is next assumed that the viscosity η is described by the new model of Equation (5). When Equation (5) for η is substituted into Equation (14) and the resulting expression is converted to dimensionless form, the following equation results:

$$-\frac{dP}{dZ}\frac{RB}{2\eta_o} = (B\gamma_R)\left[\frac{\text{arc sinh }(B\gamma_R)}{(B\gamma_R)}\right]^4 \tag{18}$$

Similarly, Equation (5) for η may be substituted into Equation (17) and the resulting expression converted to dimensionless form to obtain

$$\frac{QB}{R^3} = \frac{\pi}{3}(B\gamma_R)\left\{1 - \left[\frac{\text{arc sinh }(B\gamma_R)}{(B\gamma_R)}\right]^{3A} \int_o^1 \left[\frac{\text{arc sinh }(B\gamma_R\gamma^*)}{(B\gamma_R\gamma^*)}\right]^{3A} (\gamma^*)^3\, d\gamma^*\right\} \tag{19}$$

in which $\gamma^* = \gamma/\gamma_R$.

Equations (18) and (19) indicate that $(-dP/dZ)(RB/2\eta_o)$ and QB/R^3 are both functions of $B\gamma_R$ and A. Hence these two equations define $(-dP/dZ)(RB/2\eta_o)$ as an implicit function of QB/R^3 and A. This relationship has been determined. A numerical tabulation of $(-dP/dZ)(RB/2\eta_o)$ and QB/R^3 calculated according to Equations (18) and (19) is recorded in Table C-3 of reference *17*. Entries are given for thirty-six values of $B\gamma_R$ (at intervals of approximately 1/5 logarithmic cycle in the range $0.01 \leq B\gamma_R \leq 100{,}000$) and for fifty-one values of A (at intervals of 0.02 in the range $0 \leq A \leq 1$). In the calculation for QB/R^3, the integral was evaluated by Simpson's rule of numerical integration with a subinterval $\Delta\gamma^* = 0.05$.

The preceding numerical solution for tube flow can be put to practical use. Two applications are described below.

Prediction of Pressure Losses

Suppose that viscosity data are available and that it is desired to predict pressure losses in laminar tube flow. From Table C-3 of reference *17* a master plot of $\log\left(-\frac{dP}{dZ}\frac{RB}{2\eta_o}\right)$ vs. $\log\left(\frac{QB}{R^3}\right)$ is prepared with curves for several values of A. Such a master plot is shown in Figure 4. Parameters η_o, A, and B are determined from the viscosity data according to the procedure outlined earlier in this article. The dimensionless group QB/R^3 is next calculated for the desired flow rate Q and tube radius R. Then $(-dP/dZ)(RB/2\eta_o)$ corresponding to the known values of A and QB/R^3 is read from the master plot. Finally, since R, B, and η_o are known, one can calculate $-dP/dZ$. (A similar procedure for the Powell-Eyring model is described in reference 5.)

Determination of Viscosity Model Parameters from Tube Flow Data

Suppose now that Q vs. dP/dZ data are available and that it is desired to determine parameters η_o, A, and B. As described in the preceding paragraph, a master plot of

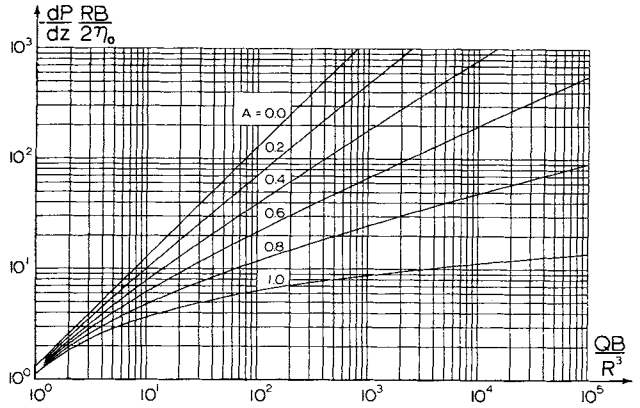

Fig. 4. Relationship between flow rate and pressure gradient for laminar flow in a cylindrical tube when the viscosity is given by Equation (5). The line for $A = 0$ represents Newtonian behavior (Poiseuille's law). Table C-3 of reference 17 contains entries for plotting nine interpolation curves between each pair of curves shown here.

$\log\left(-\frac{dP}{dZ}\frac{RB}{2\eta_o}\right)$ vs. $\log\left(\frac{QB}{R^3}\right)$ is prepared with curves for several values of A. The Q vs. dP/dZ data are plotted as $\log\left(-\frac{dP}{dZ}\frac{R}{2}\right)$ vs. $\log\left(\frac{Q}{R^3}\right)$ on a piece of graph paper with the same scale as that of the master plot. This data plot is superimposed on the master plot and moved about (keeping the coordinate axes of both plots parallel) to find the curve of the master plot which best fits the data. Parameter A is read from this curve. Parameter B is read from the abscissa on the master plot which coincides with the $Q/R^3 = 1$ abscissa on the data plot. The ratio η_o/B is read from the ordinate on the data plot which coincides with the $(-dP/dZ)(RB/2\eta_o) = 1$ ordinate on the master plot.

ACKNOWLEDGMENT

The author expresses appreciation to Professor R. Byron Bird for encouragement and guidance. Professors A. G. Fredrickson and E. B. Christiansen read the original manuscript and made helpful suggestions for improving the presentation. Financial support was provided by the Wisconsin Alumni Research Foundation, the National Science Foundation (grant G-11996), Eastman Kodak Company, and the Aerospace Research Laboratories.

NOTATION

A = parameter, Equations (5) and (6), dimensionless
B = parameter, Table 1 and Equations (5) and (6), t
d = sphere diameter, L
D = cylinder diameter, L
g = local acceleration of gravity, Lt^{-2}
K = correction to Stokes' Law, Equation (10), dimensionless
K_η = factor in Equation (8), L^{-3}
K_τ = factor in Equation (7), L^{-3}
m = parameter, Table 1, $ML^{-1}t^{n-2}$
n = parameter, Table 1, dimensionless
p = pressure, $ML^{-1}t^{-2}$
P = $p + \rho gZ\cos\beta$, $ML^{-1}t^{-2}$
Q = volumetric flow rate, L^3t^{-1}
r = cylindrical coordinate, Figure 3, L
R = tube radius, Figure 3, L
N_{Re} = Reynolds number $d\,v_t\,\rho/\eta$, dimensionless
T = torque, Equation (7), ML^2t^{-2}
v_t = terminal velocity of fall, Lt^{-1}
Z = cylindrical coordinate, Figure 3, L

Greek Letters

α = parameter, Table 1, dimensionless
β = angle defined in Figure 3, dimensionless
γ = $-\Delta$, Equation (12), t^{-1}
γ_R = γ at $r = R$, Equation (14), t^{-1}
γ^* = γ/γ_R, Equation (19), dimensionless
Δ = shear rate, Equation (4), t^{-1}
$\bar{\Delta}$ = rate of deformation tensor, Equation (1), t^{-1}
Δ_{ij} = ij^{th} component of $\bar{\Delta}$, t^{-1}
η = viscosity, Equation (1), $ML^{-1}t^{-1}$
η_s = $d^2(\rho_s - \rho)g/18\,v_t$, Equation (10), $ML^{-1}t^{-1}$
η_o = limiting viscosity at zero shear rate, $ML^{-1}t^{-1}$
η_∞ = limiting viscosity at very high shear rates, $ML^{-1}t^{-1}$
θ = cylindrical coordinate, Figure 3, dimensionless
π = 3.14159 . . .
ρ = fluid density, ML^{-3}
ρ_s = sphere density, ML^{-3}
σ = parameter, Table 1, $M^{-1}Lt^2$
τ = shear stress, Equation (4), $ML^{-1}t^{-2}$
$\bar{\tau}$ = viscous momentum flux tensor, Equation (1), $ML^{-1}t^{-2}$
τ_m = parameter, Table 1, $ML^{-1}t^{-2}$
$\tau_{1/2}$ = parameter, Table 1, $ML^{-1}t^{-2}$
Ω = angular velocity, Equation (8), t^{-1}

Special Symbols

II_Δ = second invariant of $\bar{\Delta}$, Equation (2), t^{-2}
III_Δ = third invariant of $\bar{\Delta}$, Equation (3), t^{-3}

LITERATURE CITED

1. Bacon, L. R., *J. Franklin Inst.*, **221**, 251 (1936).
2. Biery, J. C., and J. D. Huppler, *Univ. Wisconsin Eng. Expt. Sta. Rept. 19* (1962).
3. Bird, R. B., W. E. Stewart, and E. N. Lightfoot, "Transport Phenomena," 4 printing, Wiley, New York (1964).
4. Bird, R. B., *Can. J. Chem. Eng.*, **43**, 161 (1965).
5. Christiansen, E. B., N. W. Ryan, and W. E. Stevens, *A.I.Ch.E. J.*, **1**, 544 (1955).
6. Kim, W. K., N. Hirai, T. Ree, and H. Eyring, *J. Appl. Phys.*, **31**, 358 (1960).
7. Lamb, H., "Hydrodynamics," p. 599, Dover, New York (1945).
8. Lodge, A. S., "Elastic Liquids," Academic Press, New York (1964).
9. Matsuhisa, Seikichi, and R. B. Bird, *A.I.Ch.E. J.*, **11**, 588 (1965).
10. McKennell, R., *Anal. Chem.*, **28**, 1710 (1956).
11. ———, and K. Watkin, *Rheol. Acta*, **1**, 545 (1961).
12. McPherson, M. B., M.S. thesis, State Univ. Iowa, Iowa City (1947).
13. Meter, D. M., and R. B. Bird, *A.I.Ch.E. J.*, **10**, 878 (1964).
14. Reiner, M., "Deformation, Strain, and Flow," 2 ed., pp. 243, 246, Interscience, New York (1960).
15. Seely, G. R., *A.I.Ch.E. J.*, **10**, 56 (1964).
16. Slattery, J. C., *J. Colloid Sci.*, **16**, 431 (1961).
17. Sutterby, J. L., Ph.D. dissertation, Univ. Wisconsin, Madison (1964).
18. ———, *Trans. Soc. Rheol.*, **9**, No. 2 (1965).
19. Turian, R. M., Ph.D. dissertation, Univ. Wisconsin, Madison (1964).
20. ———, manuscript submitted to *Chem. Eng. Sci.*

Manuscript received December 9, 1964; revision received August 19, 1965; paper accepted August 24, 1965.